hv photonics

IMPACT FACTOR 2.536

CITESCORE 2.3

Communication

Optimally Controlled Non-Adiabatic Quantum State Transmission in the Presence of Quantum Noise

Xiang-Han Liang, Lian-Ao Wu and Zhao-Ming Wang

Special Issue

Photonic State Tomography: Methods and Applications

Edited by

Dr. Artur Czerwinski

MDPI

https://doi.org/10.3390/photonics10030274

photonics

MDPI

Communication

Optimally Controlled Non-Adiabatic Quantum State Transmission in the Presence of Quantum Noise

Xiang-Han Liang [1], Lian-Ao Wu [2,3] and Zhao-Ming Wang [1,*]

[1] College of Physics and Optoelectronic Engineering, Ocean University of China, Qingdao 266100, China
[2] Ikerbasque, Basque Foundation for Science, 48011 Bilbao, Spain
[3] Department of Physics, University of the Basque Country UPV/EHU, 48080 Bilbao, Spain
* Correspondence: wangzhaoming@ouc.edu.cn

Abstract: Pulse-controlled non-adiabatic quantum state transmission (QST) was proposed many years ago. However, in practice environmental noise inevitably damages communication quality in the proposal. In this paper, we study the optimally controlled non-adiabatic QST in the presence of quantum noise. By using the Adam algorithm, we find that the optimal pulse sequence can dramatically enhance the transmission fidelity of such an open system. In comparison with the idealized pulse sequence in a closed system, it is interesting to note that the improvement of the fidelity obtained by the Adam algorithm can even be better for a bath strongly coupled to the system. Furthermore, we find that the Adam algorithm remains powerful for different numbers of sites and different types of Lindblad operators, showing its universality in performing optimal control of quantum information processing tasks.

Keywords: non-Markovian dynamics; optimal control; Adam algorithm

Citation: Liang, X.-H.; Wu, L.-A.; Wang, Z.-M. Optimally Controlled Non-Adiabatic Quantum State Transmission in the Presence of Quantum Noise. *Photonics* **2023**, *10*, 274. https://doi.org/10.3390/photonics10030274

Received: 13 February 2023
Revised: 1 March 2023
Accepted: 2 March 2023
Published: 5 March 2023

1. Introduction

Information transfer capability lies at the heart of quantum information processing. Likewise, quantum technology requires high-fidelity QST through different locations, e.g., between remote microwave cavity memories [1], a quantum processor and quantum communication nodes [2], matter and light [3], from an ion to a photon [4], from a single photon to a distant quantum-dot electron spin [5], quantum processor and quantum communication nodes [2], velocity confinement of quantum gates, and QST in disordered one-dimensional lattices in multiple quantum bit systems [6,7]. For short-distance communication, the quantum spin chain could be a perfect candidate for a communication channel [8–11]. Numerous schemes have been suggested to realize perfect or near-perfect state transfer [8,12–14]. For example, perfect state transfer can be done by construction of the coupling structure of the chain [8,12–14]. High-fidelity QST through spin chains is made by applying an external field [15–17]. The high-fidelity QST based on the Floquet-engineered method has been proposed in the many-body problems [18].

Adiabatic evolution has been used in various quantum information processing tasks. QST based on the adiabaticity has also been suggested for years [2,16,19,20]. Recently, adiabatic QST in a semiconductor quantum-dot spin chain was studied [21] by adiabatically manipulating exchange couplings, and the spin states can be transferred between distant electrons. Typically, adiabatic QST requires a long time. However, the environmental noise will ruin the adiabaticity and this detrimental effect will increase with the evolution time [22]. Consequently, expedited adiabatic processes are desired [23,24]. Of particular interest is Ref. [25], which suggests to speedup adiabatic processes in terms of various external pulses sequences [22], specifically the acceleration of adiabatic QST in a spin chain under zero-energy-change pulse control [25]. High fidelity can be achieved with controls even in noisy environments [26–28]. Adiabatic transmission of an arbitrary entangled state

through an extended SSH chain is also discussed [29], where the topological protection can help to fight against the temporal noise caused by the imperfection in the control field.

For practical quantum state transfer, the corresponding physical communication channel will always suffer from its surrounding environmental noise. The interaction between the system and environment leads to a decrease in transmission fidelity between the idealized and the practical [30,31]. For an open system, the environment is Markovian when the memory effects can be neglected. Additionally, the Lindblad equation can be used to describe the system dynamics [32,33]. When the memory effects cannot be neglected, a non-Markovian description is necessary. The non-Markovianity of the environment has a significant influence on the open system [34,35]. For example, the memory effects of a non-Markovian environment can be applied to an opto-mechanical system to make it macroscopically entangled [36]. In general, solving the dynamics of the system in a non-Markovian environment is difficult, and the quantum state diffusion (QSD) equation is currently a newly developed method to confront this challenge [37–41]. The QST through a spin chain between two zero-temperature [37] or finite-temperature non-Markovian baths [42] has been studied using the QSD approach. The transmission fidelity decreases with the strength of the system–bath coupling and temperature.

On the other hand, besides these previous adiabatic QST proposals, Ref. [25] suggests non-adiabatic QST in terms of external pulses in a spin chain. It is interesting to note that the external pulses can somehow wash out the quasi-crossing between different energy levels during the change of the time-dependent Hamiltonian. In this paper, we will extend the protocol used in [25] to the zero-energy-cost control pulses and optimize control sequences in the presence of noise. We will use the QSD equation to investigate the non-adiabatic transport of the quantum state in a one-dimensional spin chain in the presence of noise. Zero-energy-cost control has been introduced theoretically [43] to realize almost exact state transmission in a spin chain in an open system. For the numerical optimization, we also study the stochastic learning control of adiabatic speedup in a non-Markovian open qutrit system [44]. The stochastic search procedures are proved to be powerful tools to design control pulses for combating the detrimental environment. We will compare the theoretical and numerical results for optimal pulse control in the realization of non-adiabatic QST proposals. Specifically, we will check the non-Markovian effects of the environment on the state transmission fidelity.

2. The Models and The Hamiltonian

The total Hamiltonian of the open quantum system can be written as

$$H_{tot} = H_s + H_b + H_{int}, \tag{1}$$

where H_s and H_b are the Hamiltonian of the system and bath, respectively. H_{int} is the system–bath interaction Hamiltonian. For a bosonic environment, $H_b = \Sigma_k \omega_k b_k^\dagger b_k$ (for convenience, setting $\hbar = 1$), where $b_k^\dagger$ (b_k) is the bosonic creation (annihilation) operator of kth mode with frequency ω_k. The interaction Hamiltonian H_{int} reads

$$H_{int} = \sum_k (g_k^* L^\dagger b_k + g_k L b_k^\dagger), \tag{2}$$

where g_k is the coupling strength between the system and the kth mode of the bath. L is the Lindblad operator.

Initially, suppose that the bath is prepared at the thermal equilibrium state, the density operator is $\rho(0) = e^{-\beta H_b}/Z$ with temperature T_{em}. $Z = Tr[e^{-\beta H_b}]$ is the partition function and $\beta = 1/T_{em}$ (setting $K_B = 1$). According to Refs. [17,45], the non-Markovian master equation of the system can be derived by the non-Markovian QSD equation technique [46,47].

$$\frac{\partial}{\partial t}\rho_s = -i[H_s, \rho_s] + [L, \rho_s \overline{O}_z^\dagger(t)] - [L^\dagger, \overline{O}_z(t)\rho_s]$$

$$[L^\dagger, \rho_s \overline{O}^\dagger_\omega(t)] - [L, \overline{O}_\omega(t)\rho_s], \tag{3}$$

where $\overline{O}_{z,(\omega)} = \int_0^t ds \alpha_{z,(\omega)}(t-s) O_z$, and $\alpha_{z,(\omega)}(t-s)$ is the bath correlation function. The quantum master equation is a time-convolutionless form truncated from the environmental correlations [48,49]. Note that in the above equation, the weak coupling is assumed and the O operators are assumed to be independent of noises [50].

For the bath we choose the Lorentz spectrum, with the spectral density $J(\omega) = \frac{\Gamma}{\pi} \frac{\omega}{1+(\frac{\omega}{\gamma})^2}$, where Γ and γ are real parameters, γ represents the characteristic frequency of the bath, and Γ represents the strength of the system–bath coupling. With the Lorentz spectrum, the bath correlation functions can be written as

$$\alpha_z(t-s) = \Gamma T_{em} \Lambda(t,s) + i\Gamma \Lambda(t,s), \tag{4}$$

$$\alpha_\omega(t-s) = \Gamma T_{em} \Lambda(t,s), \tag{5}$$

where $\Lambda(t,s) = \frac{\gamma}{2} e^{-\gamma|t-s|}$ is an Ornstein–Uhlenbeck correlation function. $1/\gamma$ represents the memory time of the environment. For Equations (4) and (5), we have the relations,

$$\frac{\partial \alpha_{z(\omega)}(t-s)}{\partial t} = -\gamma \alpha_{z(\omega)}(t-s). \tag{6}$$

The $\overline{O}_{z,(\omega)}$ operator satisfies [47,51],

$$\frac{\partial \overline{O}_z}{\partial t} = (\frac{\Gamma T_{em} \gamma}{2} - \frac{i\Gamma\gamma^2}{2})L - \gamma \overline{O}_z + [-iH_s - (L^\dagger \overline{O}_z + L\overline{O}_\omega), \overline{O}_z], \tag{7}$$

$$\frac{\partial \overline{O}_\omega}{\partial t} = \frac{\Gamma T_{em} \gamma}{2} L^\dagger - \gamma \overline{O}_\omega + [-iH_s - (L^\dagger \overline{O}_z + L\overline{O}_\omega), \overline{O}_\omega]. \tag{8}$$

In the Markov limit, Equations (4) and (5) become $\alpha_z(t-s) = \alpha_\omega(t-s) = \Gamma T_{em} \delta(t-s)$. $\overline{O}_z = \frac{\Gamma T_{em}}{2} L$ and $\overline{O}_\omega = \frac{\Gamma T_{em}}{2} L^\dagger$. The master equation in Equation (3) reduces to the Lindblad form [39,42,46,51],

$$\begin{aligned} \frac{\partial}{\partial t}\rho_s = -i[H_s, \rho_s] + \frac{\Gamma T_{em}}{2}[(2L\rho_s L^\dagger - L^\dagger L \rho_s - \rho_s L^\dagger L) \\ + (2L^\dagger \rho_s L - LL^\dagger \rho_s - \rho_s LL^\dagger)]. \end{aligned} \tag{9}$$

For the system Hamiltonian, in this paper we choose the time-dependent one-dimensional spin chain model as in Ref. [25],

$$H_s(t) = A(t) H_{xy} + B(t) H_z, \tag{10}$$

where $H_{xy} = J \sum_{i=1}^{N-1} (\sigma_i^x \sigma_{i+1}^x + \sigma_i^y \sigma_{i+1}^y)$ is the hopping term, and $H_z = \sum_{i=1}^N h(i) \sigma_i^z$ is the on-site energy term. J represents the coupling between the nearest two sites, and now we set $J = -1.0$ throughout. N is the number of sites. $\sigma_i^x, \sigma_i^y, \sigma_i^z$ are the Pauli matrices acting on spin i. i is the location of the sites, $i = 1, 2, \ldots, N$. $h(i)$ represents a non-zero gradient field along the z-direction of the spin chain [25,52]. For $h(i)$, $h(i) < h(i+1)$. T is the total evolution time. For $A(t)$ and $B(t)$, they satisfy the conditions $A(0) = A(T) = 0$ and $B(0) = 1$, $B(T) = -1$. For simplicity, let $h(i) = h_m i$. This model can be realized in an optics lattice [53,54]. In this case, $A(t) = sin(\Omega t)$, $B(t) = cos(\Omega t)$, and $\Omega = \pi/T$. The model physically describes ultracold atoms in a one-dimensional optical lattice modulated by laser beam [55].

Now suppose the initial state of the system is prepared as $|\Phi_s(0)\rangle = |1\cdots00\rangle$. The target is to transfer the state $|1\rangle$ at the first site to the other end of the chain at some time T with $|\Phi_s(T)\rangle = |0\cdots01\rangle$. The fidelity can be defined as

$$F(t) = \sqrt{\langle\Phi_s(T)|\rho_s(t)|\Phi_s(T)\rangle}, \tag{11}$$

where $\rho_s(t)$ is the system's reduced density matrix obtained in Equation (3).

3. Quantum State Transfer under Control

Normally, the existence of the environmental noise will destroy the quantum information processing tasks, e.g., decreasing the state transmission fidelity [42] or adiabaticity [44]. Quantum control has been applied to resist the detrimental effects of the environment. A recursive method [56] has been used to calculate the state transmission fidelity of arbitrary-length X-X spin chains boundary-driven by non-Markovian environments. Quantum optimal control [57] by adding a leakage elimination operator Hamiltonian to the system [44] has been suggested to realize adiabatic speedup in a non-Markovian open qutrit system. The leakage elimination operator Hamiltonian can be realized by a sequence of pulses, which can be constructed as [22,58,59]

$$H(t) = [1 + c(t)]H_0(t), \tag{12}$$

where $c(t)$ represents the control function. In Ref. [25], $c(t)$ is chosen to be an arbitrary function but always positive, as a result, the system average energy will be increased. In this paper, the pulse is chosen as a zero area pulse as in Ref. [17,44] with a positive in the first half period and a negative in the second half period. In this case, the average energy of the system is not increased. Additionally, the type of the pulses has little influence on the fidelity [60], so we take the rectangular pulse as an example [61,62]:

$$c(t) = \begin{cases} I, 2n\tau < t < (2n+1)\tau, \\ -I, (2n+1)\tau < t < (2n+2)\tau, \end{cases} \tag{13}$$

where $n = 0, 1, 2, \ldots$, I is the pulse strength and τ is half period of the pulses. For this kind of pulse, it has been theoretically derived that if the pulses satisfy the condition $I\tau = 2\pi m$, $m = 1, 2, 3, \ldots$ [22,59,63], the adiabatic speedup can be realized. Note that this condition is only valid for a fixed energy gap and closed system. In our model, the energy gap $\triangle E_{01}$ between the ground state and the first excited state is time-dependent. In this case, the pulse strength can be tuned as $I(t) = I/\triangle E_{01}$ [63,64]. In our model, the energy level crossing occurs at $t = T/2$, which leads to an infinite pulse intensity at that point. We then use a suitable value instead at the crossing point. The Lindblad operation $L = \Sigma_i \sigma_i^-$ is used if not especially specified. $\sigma_i^- = \sigma_i^x - i\sigma_i^y$ is the spin lowering operator.

In Figure 1, we plot the fidelity as a function of the rescaled time t/T with and without control. For the control, the ideal pulse condition $I\tau = 2\pi$ is used with $I = 20$, $\tau = \pi/10$. If we do not consider the environment ($\Gamma = 0$), the ideal pulse control can be used to dramatically improve the fidelity. Near-perfect QST ($F = 0.99837$) can be obtained at $t/T = 1$. However, when considering the environment ($\Gamma = 0.01$), the fidelity is low even under control ($F = 0.56041$).

We have stressed that the ideal pulse conditions are derived for a closed system. Now from Figure 1, we see that it loses its effectiveness in an open system. Stochastic learning control of adiabatic speedup in a non-Markovian open qutrit system has been studied in Ref. [44]. The stochastic search procedures are proved to be powerful tools for the design of control pulses in an open system. Here we will use the Adam algorithm [65], which is the extended version of stochastic gradient descent, to design the optimal pulse for high-fidelity state transmission in the presence of an environment.

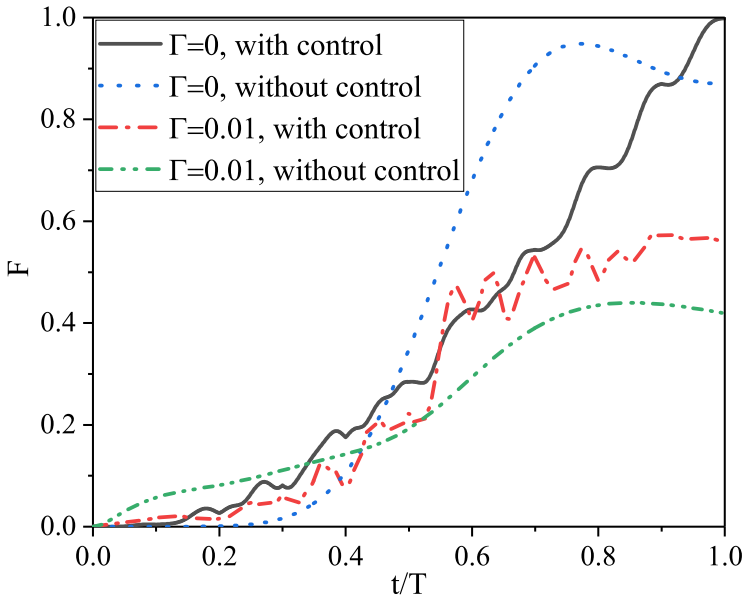

Figure 1. The fidelity F versus the rescaled time t/T. The total evolution time $T = \pi$. With control the parameters $I = 20, \tau = \pi/10$. In the presence of an environment, the parameters are taken as $\Gamma = 0.01, \gamma = 20, Tem = 20$. The number of sites $N = 5$.

Now the optimization objective can be denoted as minimizing the loss function, or fidelity error. It is usually defined as

$$Loss(I^N) = 1 - F(I^N) + \lambda c_{max}. \tag{14}$$

Here c_{max} is the maximum value of the control function $c(t)$. λ is a constant, in this paper we choose $\lambda = 0.01$. We introduce this term to constrain the control pulse. Equation (14) allows for the competition between the infidelity $1 - F(I^N)$ and the maximum applied control intensity c_{max}, thus avoiding the generation of an optimized pulse with too large intensity.

The Adam algorithm can be denoted as follows.

Step 1. Calculate the gradient vector $\boldsymbol{g}$ of the loss function *Loss* with respect to the selected variable $\boldsymbol{I}$

$$\boldsymbol{g} = \nabla_{\boldsymbol{I}} Loss(\boldsymbol{I}). \tag{15}$$

Step 2. Calculate the new exponential moving average

$$\boldsymbol{m} = \beta_1 \boldsymbol{m} + (1 - \beta_1)\boldsymbol{g}. \tag{16}$$

$$\boldsymbol{v} = \beta_2 \boldsymbol{v} + (1 - \beta_2)(\boldsymbol{g})^2. \tag{17}$$

Step 3. Compute the new bias-corrected moment vectors

$$\hat{\boldsymbol{m}} = \boldsymbol{m}/(1 - \beta_1). \tag{18}$$

$$\hat{\boldsymbol{v}} = \boldsymbol{v}/(1 - \beta_2). \tag{19}$$

Step 4. Update the variables $\boldsymbol{I}$ according to

$$\boldsymbol{I} = \boldsymbol{I} - \alpha \hat{\boldsymbol{m}}/(\sqrt{\hat{\boldsymbol{v}}} + \varepsilon). \tag{20}$$

Step 5. Repeat the above steps until $Loss < \xi$ or $k > k_{max}$ (ξ and k_{max} denote the given threshold and the maximum number of iterations, respectively).

For the Adam algorithm, $\boldsymbol{I}$ indicates pulse intensity, $\boldsymbol{g}$ is the gradient, β is a fixed parameter, α is the learning rate, and ε is a constant set to avoid the denominator being zero. ξ is the given threshold.

The complete algorithm description of Adam is shown in (Algorithm 1).

Algorithm 1 Adam.

Initial pulse intensity $\boldsymbol{I^i}$.
Parameter: EMA parameters β_1 and β_2, learning rate α and the epsilon ε.
for iteration $k = 1, k_{max}, \boldsymbol{m^i} = 0, \boldsymbol{v^i} = 0$.

- Randomly choose a spin pulse.
- Calculate the gradient $\boldsymbol{g^k} = \bigtriangledown_{\boldsymbol{I^k}} Loss(\boldsymbol{I^k})$.
- Calculate the exponential moving averages
  $\boldsymbol{m^k} = \beta_1 \boldsymbol{m^{k-1}} + (1-\beta_1)\boldsymbol{g^k}$,
  $\boldsymbol{v^k} = \beta_2 \boldsymbol{v^{k-1}} + (1-\beta_2)(\boldsymbol{g^k})^2$.
- Calculate the bias-corrected moment vectors.
  $\hat{\boldsymbol{m^k}} = \boldsymbol{m^k}/[1-(\beta_1)^k], \hat{\boldsymbol{v^k}} = \boldsymbol{v^k}/[1-(\beta_2)^k]$
- Update the pulse $\boldsymbol{I^k} = \boldsymbol{I^{k-1}} - \alpha \hat{\boldsymbol{m^k}}/(\sqrt{\hat{\boldsymbol{v^k}}} + \varepsilon)$.
- **Break** if $1 - F(J^N) < \xi$ or $k > k_{max}$.

end for

The selection of the initial control pulse $I(t)$ is either by experience or guessing. β_1 (β_2) is the decay exponent of the first (second) moment estimate. This method is computationally efficient and requires less memory. By updating $\boldsymbol{g_t}, \boldsymbol{m_t}, \boldsymbol{v_t}$, we can optimize the pulses to improve the fidelity. The iteration is terminated if the loss function $Loss(I^k)$ after the iteration is less than a given threshold ξ ($\xi = 0.001$) or the iteration times $k > k_{max}$. If the fidelity F is improved, we keep the updated pulse I^k. Otherwise, we discard it. In this way, the pulse I is gradually optimized and finally, the optimal solution is obtained.

We first check the effectiveness of the Adam. In Figure 2 we plot the convergence behavior of the algorithm. In the optimization, we set the final fidelity F to 0.999, correspondingly the parameter $\xi = 0.001$. As an example, the environmental parameters are taken as $\Gamma = 0.003, 0.005, 0.007$, $\gamma = 2$, $Tem = 10$, $T = \pi$, $N = 5$, and $\tau = \pi/10$. In this case, the learning rate α in the Adam algorithm is chosen to be 1, parameters $\beta_1 = 0.9$ and $\beta_2 = 0.999$.

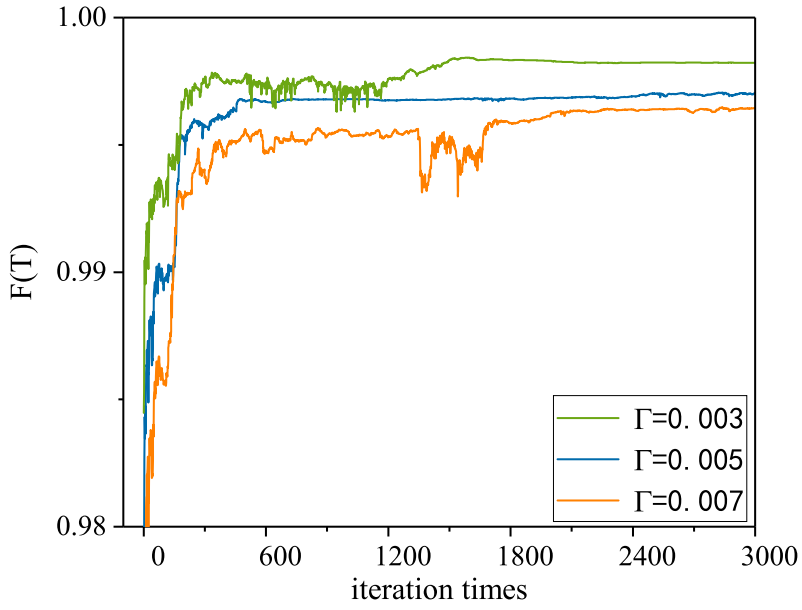

Figure 2. The variation of the fidelity $F(T)$ vs the number of iteration times for different Γ. $\gamma = 2$ and $Tem = 10$.

From Figure 2 we see that the algorithm converges quickly: after about 3000 iterations the steady value is obtained. Therefore, the maximum number of iterations of 3000 is chosen in this paper. We also find that when Γ becomes larger, the final fidelity $F(T)$ is smaller, which will be discussed later.

4. Results and Discussion

In this section, we will use the Adam algorithm to design the zero-area pulses for high-fidelity non-adiabatic QST. We will also compare the performances of the ideal pulses which are derived from the closed system [20,60] and Adam-optimized pulses. We use the rectangular pulses as in Equation (13) and define them as ideal pulses. For Adam-optimized pulses, we take $I = 10$ as our initial guess, which is different from the ideal pulses.

At first, we analyze the effects of the environment on transmission fidelity. In Figure 3, we plot the final fidelity $F(T)$ via Adam optimization as a function of the environmental parameters Γ, γ, and T, respectively. To show the performance of the control, we also plot $F(T)$ without the control. Clearly, the optimal pulses designed by the Adam algorithm show its effectiveness: the near-perfect QST can be realized even for a stronger bath (bigger Γ, Tem, and γ). From Figure 3b, $F(T)$ decreases with increasing γ, this is in accordance with previous results: a non-Markovian bath will be helpful to realize an effective transmission control that the fidelity can be boosted [43]. We also plot the pulse intensity $I(t)$ as a function of the rescaled time t/T in Figure 3c. For the ideal pulses, $I(t)$ is tuned by the energy gap. Although the intensities of the Adam pulses are different in different periods, it is constant in the half period. So the Adam pulses might be easier to realize in the experiment.

To show the superiority of the Adam pulses to the ideal pulses, we calculate the fidelity improvement Im, which is defined by

$$Im = F(T)^{Adam} - F(T)^{ideal}. \tag{21}$$

where $F(T)^{Adam}$ and $F(T)^{ideal}$ are the final fidelity obtained from the Adam pulses and the ideal pulses, respectively.

Figure 4 plots the fidelity improvement Im for different environemntal parameters Γ, Tem, and γ, respectively. For different Γ, $\gamma = 2, Tem = 10$. For different γ, $\Gamma = 0.04$, $Tem = 10$. For different Tem, $\Gamma = 0.005, \gamma = 2$. From Figure 4a, Im increases with increasing Γ or Tem. A stronger bath will destroy the system more and as a result, the idea pulses lose their effectiveness because it is only valid in a closed system. Then the Adam algorithm shows its advantage in an open system. Figure 4b shows that Im first increases then decreases with increasing γ. That is to say, for a more Markovian bath, the control loses its effectiveness for both Adam and ideal pulses, then Im correspondingly becomes smaller. The inset plot in Figure 4b shows the variation of fidelity with time for the three cases in the Markov limit. The final fidelity after optimization of the Adam algorithm is $F(T) = 0.4472$. The fidelities under ideal pulse and without control are $F(T) = 0.4388$ and $F(T) = 0.4029$, respectively. In the Markovian limit, the control is ineffective and Im tends to be zero [43]. In sum, once the environmental parameters are ascertained, the corresponding pulses can be designed.

We only consider a fixed number of sites $N = 5$ and the Lindblad operator $L = \Sigma_i \sigma_i^-$ in our previous discussion. Next, we consider different N and L. Figure 5a plots $F(T)$ versus N for ideal pulses and Adam pulses. As expected, $F(T)$ decreases with increasing N. However, the fidelity obtained by Adam pulses is always higher than the ideal case. For the Adam pulses, $F(T)$ decreases slowly with increasing N. Figure 5b plots the time evolution of the fidelity F for $L = \Sigma_i \sigma_i^-$, $\Sigma_i \sigma_i^x$ and $\Sigma_i \sigma_i^z$ with Adam and ideal pulses. The fidelity improvement of the Adam pulses can still be obtained for different L. In other words, the control scheme is still powerful. For $L = \Sigma_i \sigma_i^z$, the final fidelity $F(T)$ with Adam pulses is the biggest, $L = \Sigma_i \sigma_i^-$ is in the middle, and $L = \Sigma_i \sigma_i^x$ is the smallest.

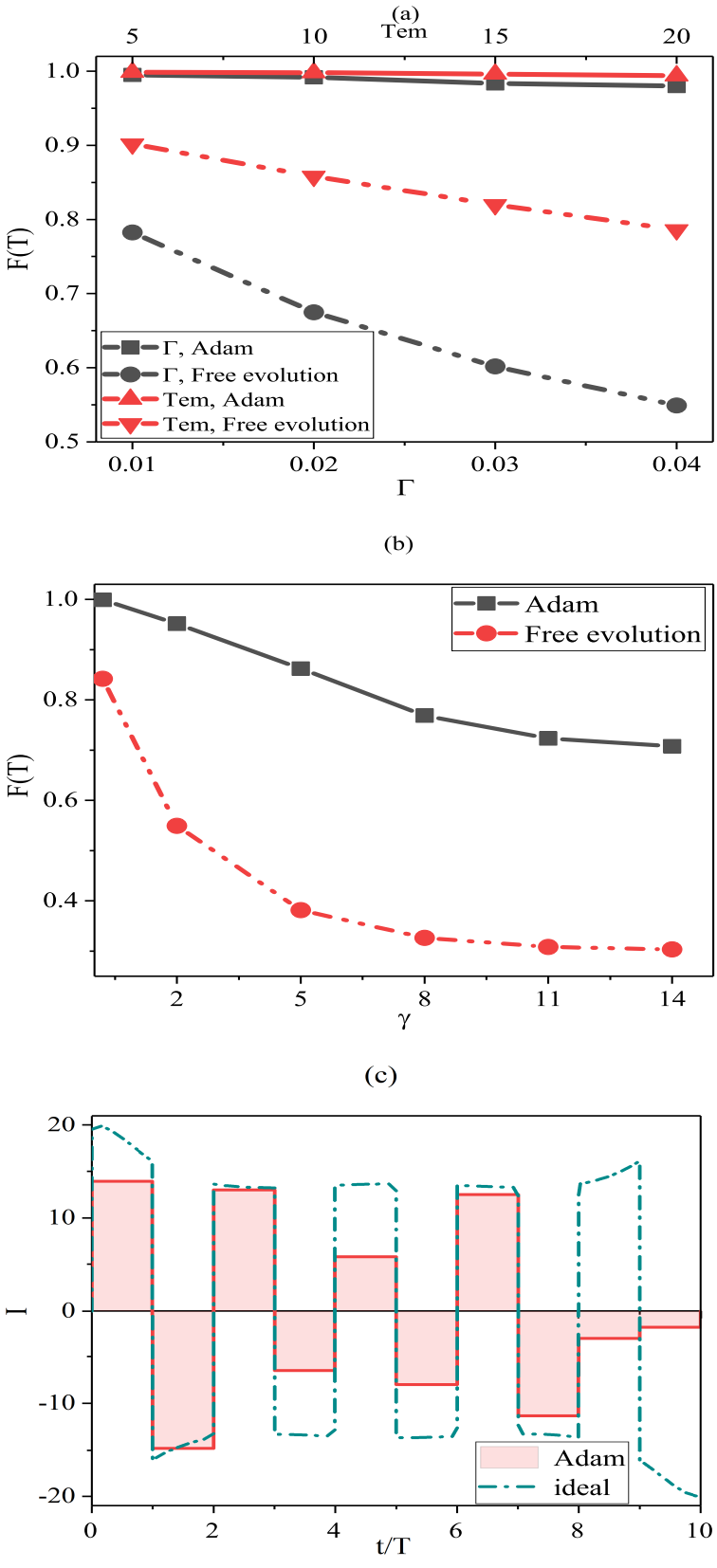

Figure 3. The fidelity $F(T)$ with and without optimal pulses for different parameters. Only one environmental parameter is changed per line, the rest of the environmental parameters are the same. $L = \Sigma_i \sigma_i^-$. (**a**) $\gamma = 2, Tem = 10$ for Γ. $\Gamma = 0.005, \gamma = 2$ for Tem. (**b**) $\Gamma = 0.04, Tem = 10$ for γ. (**c**) The profile of the ideal pulses and Adam pulses. The environmental parameters $\Gamma = 0.04, \gamma = 14$, and $Tem = 10$.

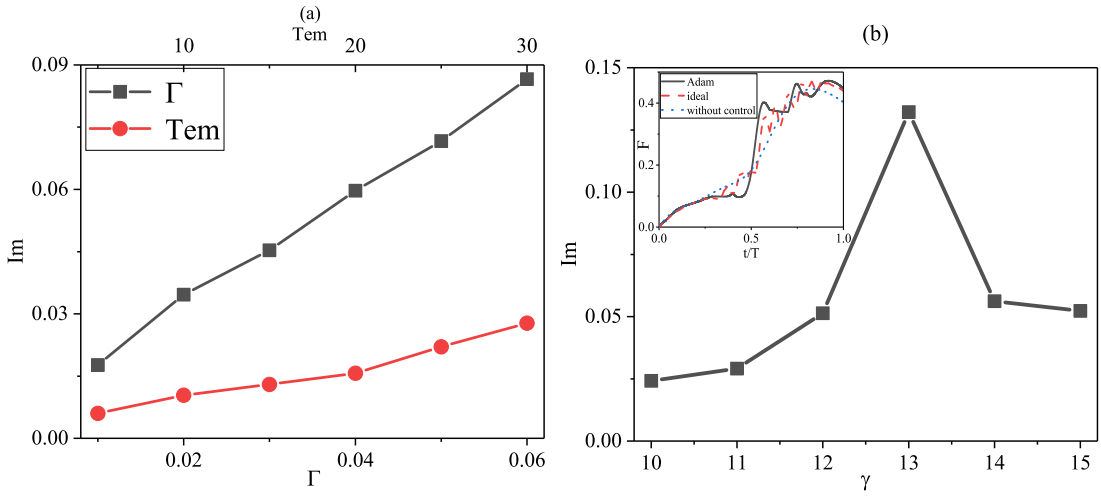

Figure 4. The fidelity improvement Im for different environmental parameters. $L = \Sigma_i \sigma_i^-$. (**a**) Γ and Tem. For different Γ, $\gamma = 2$, $Tem = 10$. For different Tem, $\Gamma = 0.005$, $\gamma = 2$. (**b**) γ. $\Gamma = 0.04$, $Tem = 10$.

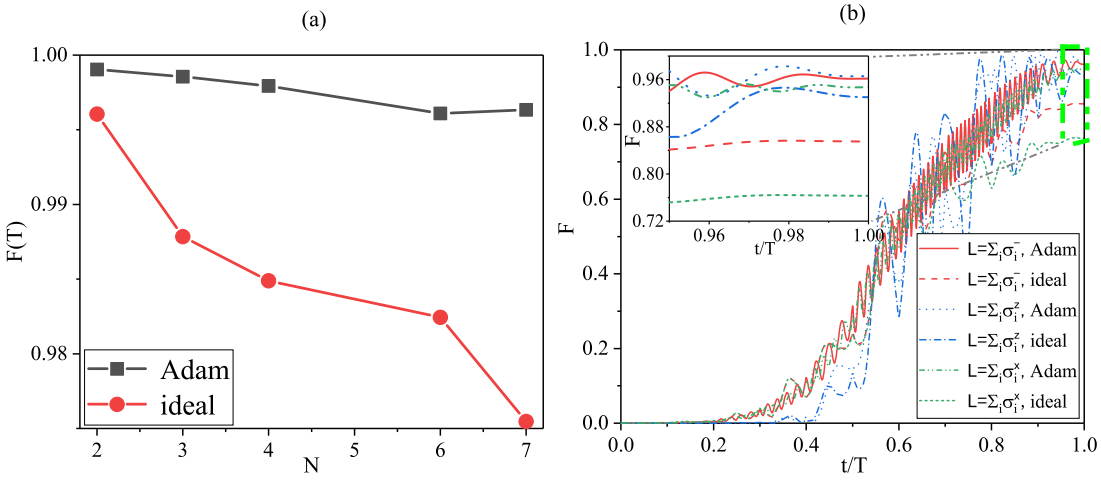

Figure 5. (**a**) Variation of the fidelity $F(T)$ vs the number of sites. Here $\Gamma = 0.005, \gamma = 2$, and $Tem = 10$. (**b**) Change in fidelity F vs time t/T with the ideal pulses and the Adam pulses when $L = \Sigma_i \sigma_i^-, \Sigma_i \sigma_i^z, \Sigma_i \sigma_i^x$. $N = 5, \Gamma = 0.01, \gamma = 8, Tem = 15$.

5. Conclusions

Optimal control has been widely applied in different fields of physics. In this paper, we use the Adam algorithm, the extended version of the stochastic gradient descent algorithm, to find the optimal pulses for the enhancement of the non-adiabatic QST fidelity in a non-Markovian environment. The model is a time-dependent one-dimensional spin chain in a finite-temperature heat bath. We use the non-Markovian quantum master equation, which is derived from the QSD technique, to calculate the dynamics of the chain. We find that the state transmission fidelity can be dramatically enhanced by the Adam pulses. Furthermore, we compare two kinds of pulses: Adam pulses and ideal pulses. Though the fidelity can be enhanced by the ideal pulses, it is always lower than the Adam pulses because it is only valid in a closed system. The fidelity improvement Im for these two cases (Γ and γ) becomes larger for a stronger bath, demonstrating the advantage of the Adam algorithm. Furthermore, we consider different lengths of the chain and types of the Lindblad operator. Our calculation results show that the Adam algorithm is still effective. Our investigation shows that the optimal control algorithm is a powerful tool to design pulses in performing quantum information processing tasks.

Author Contributions: Conceptualization, Z.-M.W. and L.-A.W.; methodology, X.-H.L. and Z.-M.W.; validation Z.-M.W. and L.-A.W.; writing—original draft preparation, X.-H.L.; writing—review and editing, Z.-M.W. and L.-A.W.; supervision, Z.-M.W. All authors have read and agreed to the published version of the manuscript.

Funding: This work was supported by the Natural Science Foundation of Shandong Province (Grant No. ZR2021LLZ004), the Natural Science Foundation of China (Grant No. 11475160), the Spanish Grant No. PID2021- 126273NB- I00 funded by MCIN/AEI/10.13039/501100011033 and by "ERDF A way of making Europe", and the Basque Government through Grant No. IT1470-22.

Institutional Review Board Statement: Not applicable.

Informed Consent Statement: Not applicable.

Data Availability Statement: The datasets used and/or analyzed during the current study are available from the corresponding author upon reasonable request.

Acknowledgments: We would like to thank Yang-Yang Xie, Arapat Ablimit, and Run-Hong He for their helpful discussions.

Conflicts of Interest: The authors declare no conflict of interest.

Abbreviations

The following abbreviations are used in this manuscript:

QST	Quantum State Transmission
QSD	Quantum State Diffusion
EMA	Exponential Moving Average

References

1. Axline, C.J.; Burkhart, L.D.; Pfaff, W.; Zhang, M.; Chou, K.; Campagne-Ibarcq, P.; Reinhold, P.; Frunzio, L.; Girvin, S.; Jiang, L.; et al. On-demand quantum state transfer and entanglement between remote microwave cavity memories. *Nat. Phys.* **2018**, *14*, 705–710. [CrossRef]
2. Chapman, R.J.; Santandrea, M.; Huang, Z.; Corrielli, G.; Crespi, A.; Yung, M.H.; Osellame, R.; Peruzzo, A. Experimental perfect state transfer of an entangled photonic qubit. *Nat. Commun.* **2016**, *7*, 11339. [CrossRef] [PubMed]
3. Matsukevich, D.; Kuzmich, A. Quantum state transfer between matter and light. *Science* **2004**, *306*, 663–666. [CrossRef]
4. Stute, A.; Casabone, B.; Brandstätter, B.; Friebe, K.; Northup, T.; Blatt, R. Quantum-state transfer from an ion to a photon. *Nat. Photonics* **2013**, *7*, 219–222. [CrossRef] [PubMed]
5. He, Y.; He, Y.M.; Wei, Y.J.; Jiang, X.; Chen, K.; Lu, C.Y.; Pan, J.W.; Schneider, C.; Kamp, M.; Höfling, S. Quantum state transfer from a single photon to a distant quantum-dot electron spin. *Phys. Rev. Lett.* **2017**, *119*, 060501. [CrossRef] [PubMed]
6. Ashhab, S. Quantum state transfer in a disordered one-dimensional lattice. *Phys. Rev. A* **2015**, *92*, 062305. [CrossRef]
7. Ashhab, S.; De Groot, P.; Nori, F. Speed limits for quantum gates in multiqubit systems. *Phys. Rev. A* **2012**, *85*, 052327. [CrossRef]
8. Christandl, M.; Datta, N.; Ekert, A.; Landahl, A.J. Perfect State Transfer in Quantum Spin Networks. *Phys. Rev. Lett.* **2004**, *92*, 187902. [CrossRef]
9. Apollaro, T.J.G.; Banchi, L.; Cuccoli, A.; Vaia, R.; Verrucchi, P. 99%-fidelity ballistic quantum-state transfer through long uniform channels. *Phys. Rev. A* **2012**, *85*, 052319. [CrossRef]
10. Bayat, A.; Banchi, L.; Bose, S.; Verrucchi, P. Initializing an unmodulated spin chain to operate as a high-quality quantum data bus. *Phys. Rev. A* **2011**, *83*, 062328. [CrossRef]
11. Lorenzo, S.; Apollaro, T.J.G.; Paganelli, S.; Palma, G.M.; Plastina, F. Transfer of arbitrary two-qubit states via a spin chain. *Phys. Rev. A* **2015**, *91*, 042321. [CrossRef]
12. Christandl, M.; Datta, N.; Dorlas, T.C.; Ekert, A.; Kay, A.; Landahl, A.J. Perfect transfer of arbitrary states in quantum spin networks. *Phys. Rev. A* **2005**, *71*, 032312. [CrossRef]
13. Kay, A. Perfect state transfer: Beyond nearest-neighbor couplings. *Phys. Rev. A* **2006**, *73*, 032306. [CrossRef]
14. Zhang, X.M.; Cui, Z.W.; Wang, X.; Yung, M.H. Automatic spin-chain learning to explore the quantum speed limit. *Phys. Rev. A* **2018**, *97*, 052333. [CrossRef]
15. Fitzsimons, J.; Twamley, J. Globally controlled quantum wires for perfect qubit transport, mirroring, and computing. *Phys. Rev. Lett.* **2006**, *97*, 090502. [CrossRef]
16. Balachandran, V.; Gong, J. Adiabatic quantum transport in a spin chain with a moving potential. *Phys. Rev. A* **2008**, *77*, 012303. [CrossRef]
17. Wang, Z.M.; Ren, F.H.; Sarandy, M.S.; Byrd, M.S. Nonequilibrium quantum thermodynamics in non-Markovian adiabatic speedup. *Phys. A Stat. Mech. Its Appl.* **2022**, *603*, 127861. [CrossRef]

18. Zhou, H.; Chen, X.; Nie, X.; Bian, J.; Ji, Y.; Li, Z.; Peng, X. Floquet-engineered quantum state transfer in spin chains. *Sci. Bull.* **2019**, *64*, 888–895. [CrossRef] [PubMed]
19. Chancellor, N.; Haas, S. Using the J1–J2 quantum spin chain as an adiabatic quantum data bus. *New J. Phys.* **2012**, *14*, 095025. [CrossRef]
20. Chen, Y.; Zhang, L.; Gu, Y.; Wang, Z.M. Acceleration of adiabatic quantum state transfer in a spin chain under zero-energy-change pulse control. *Phys. Lett. A* **2018**, *382*, 2795–2798. [CrossRef]
21. Kandel, Y.P.; Qiao, H.; Fallahi, S.; Gardner, G.C.; Manfra, M.J.; Nichol, J.M. Adiabatic quantum state transfer in a semiconductor quantum-dot spin chain. *Nat. Commun.* **2021**, *12*, 2156. [CrossRef]
22. Wang, Z.M.; Luo, D.W.; Byrd, M.S.; Wu, L.A.; Yu, T.; Shao, B. Adiabatic speedup in a non-Markovian quantum open system. *Phys. Rev. A* **2018**, *98*, 062118. [CrossRef]
23. Guéry-Odelin, D.; Ruschhaupt, A.; Kiely, A.; Torrontegui, E.; Martínez-Garaot, S.; Muga, J.G. Shortcuts to adiabaticity: Concepts, methods, and applications. *Rev. Mod. Phys.* **2019**, *91*, 045001. [CrossRef]
24. Luan, T.; Shen, H.; Yi, X. Shortcuts to adiabaticity with general two-level non-Hermitian systems. *Phys. Rev. A* **2022**, *105*, 013714. [CrossRef]
25. Wang, Z.M.; Bishop, C.A.; Jing, J.; Gu, Y.J.; Garcia, C.; Wu, L.A. Shortcut to nonadiabatic quantum state transmission. *Phys. Rev. A* **2016**, *93*, 062338. [CrossRef]
26. Oh, S.; Lee, S.; Lee, H.w. Fidelity of quantum teleportation through noisy channels. *Phys. Rev. A* **2002**, *66*, 022316. [CrossRef]
27. Xue, C.; Chen, Z.Y.; Wu, Y.C.; Guo, G.P. Effects of quantum noise on quantum approximate optimization algorithm. *Chin. Phys. Lett.* **2021**, *38*, 030302. [CrossRef]
28. Benabdallah, F.; Rahman, A.U.; Haddadi, S.; Daoud, M. Long-time protection of thermal correlations in a hybrid-spin system under random telegraph noise. *Phys. Rev. E* **2022**, *106*, 034122. [CrossRef]
29. Wang, C.; Li, L.; Gong, J.; Liu, Y.X. Arbitrary entangled state transfer via a topological qubit chain. *Phys. Rev. A* **2022**, *106*, 052411. [CrossRef]
30. Jeske, J.; Vogt, N.; Cole, J.H. Excitation and state transfer through spin chains in the presence of spatially correlated noise. *Phys. Rev. A* **2013**, *88*, 062333. [CrossRef]
31. Chen, X.; Mereau, R.; Feder, D.L. Asymptotically perfect efficient quantum state transfer across uniform chains with two impurities. *Phys. Rev. A* **2016**, *93*, 012343. [CrossRef]
32. Breuer, H.P.; Petruccione, F. *The Theory of Open Quantum Systems*; Oxford University Press on Demand: New York, NY, USA, 2002.
33. Hu, M.L. State transfer in dissipative and dephasing environments. *Eur. Phys. J. D* **2010**, *59*, 497–507. [CrossRef]
34. Breuer, H.P.; Laine, E.M.; Piilo, J.; Vacchini, B. Colloquium: Non-Markovian dynamics in open quantum systems. *Rev. Mod. Phys.* **2016**, *88*, 021002. [CrossRef]
35. De Vega, I.; Alonso, D. Dynamics of non-Markovian open quantum systems. *Rev. Mod. Phys.* **2017**, *89*, 015001. [CrossRef]
36. Zhao, X. Macroscopic entanglement in optomechanical system induced by non-Markovian environment. *Opt. Express* **2019**, *27*, 29082–29097. [CrossRef]
37. Ren, F.H.; Wang, Z.M.; Gu, Y.J. Quantum state transfer through a spin chain in two non-Markovian baths. *Quantum Inf. Process.* **2019**, *18*, 193. [CrossRef]
38. Shi, W.; Zhao, X.; Yu, T. Non-Markovian fermionic stochastic Schrödinger equation for open system dynamics. *Phys. Rev. A* **2013**, *87*, 052127. [CrossRef]
39. Yu, T.; Diósi, L.; Gisin, N.; Strunz, W.T. Non-Markovian quantum-state diffusion: Perturbation approach. *Phys. Rev. A* **1999**, *60*, 91. [CrossRef]
40. Li, C.F.; Guo, G.C.; Piilo, J. Non-Markovian quantum dynamics: What is it good for? *EPL (Europhys. Lett.)* **2020**, *128*, 30001. [CrossRef]
41. Nakajima, T.; Delbecq, M.R.; Otsuka, T.; Amaha, S.; Yoneda, J.; Noiri, A.; Takeda, K.; Allison, G.; Ludwig, A.; Wieck, A.D.; et al. Coherent transfer of electron spin correlations assisted by dephasing noise. *Nat. Commun.* **2018**, *9*, 2133. [CrossRef]
42. Wang, Z.M.; Ren, F.H.; Luo, D.W.; Yan, Z.Y.; Wu, L.A. Quantum state transmission through a spin chain in finite-temperature heat baths. *J. Phys. A Math. Theor.* **2021**, *54*, 155303. [CrossRef]
43. Wang, Z.M.; Ren, F.H.; Luo, D.W.; Yan, Z.Y.; Wu, L.A. Almost-exact state transfer by leakage-elimination-operator control in a non-Markovian environment. *Phys. Rev. A* **2020**, *102*, 042406. [CrossRef]
44. Xie, Y.Y.; Ren, F.H.; He, R.H.; Ablimit, A.; Wang, Z.M. Stochastic learning control of adiabatic speedup in a non-Markovian open qutrit system. *Phys. Rev. A* **2022**, *106*, 062612. [CrossRef]
45. Nie, S.S.; Ren, F.H.; He, R.H.; Wu, J.; Wang, Z.M. Control cost and quantum speed limit time in controlled almost-exact state transmission in open systems. *Phys. Rev. A* **2021**, *104*, 052424. [CrossRef]
46. Diósi, L.; Strunz, W.T. The non-Markovian stochastic Schrödinger equation for open systems. *Phys. Lett. A* **1997**, *235*, 569–573. [CrossRef]
47. Diósi, L.; Gisin, N.; Strunz, W.T. Non-Markovian quantum state diffusion. *Phys. Rev. A* **1998**, *58*, 1699. [CrossRef]
48. Cai, X.; Zheng, Y. Non-Markovian decoherence dynamics in nonequilibrium environments. *J. Chem. Phys.* **2018**, *149*, 094107.
49. Shibata, F.; Arimitsu, T. Expansion formulas in nonequilibrium statistical mechanics. *J. Phys. Soc. Jpn.* **1980**, *49*, 891–897. [CrossRef]

50. Xu, J.; Zhao, X.; Jing, J.; Wu, L.A.; Yu, T. Perturbation methods for the non-Markovian quantum state diffusion equation. *J. Phys. Math. Theor.* **2014**, *47*, 435301. [CrossRef]
51. Yu, T. Non-Markovian quantum trajectories versus master equations: Finite-temperature heat bath. *Phys. Rev. A* **2004**, *69*, 062107. [CrossRef]
52. Chen, B.; Fan, W.; Xu, Y.; Peng, Y.D.; Zhang, H.Y. Multipath adiabatic quantum state transfer. *Phys. Rev. A* **2013**, *88*, 022323. [CrossRef]
53. Feng, Z.; Gao, Z.W.; Wu, L.A.; Tang, H.; Sun, K.; Hu, C.Q.; Wang, Y.; Li, Z.M.; Wang, X.W.; Chen, Y.; et al. Photonic Newton's cradle for remote energy transport. *Phys. Rev. Appl.* **2019**, *11*, 044009. [CrossRef]
54. Wu, L.A.; Lidar, D.A. Overcoming quantum noise in optical fibers. *Phys. Rev. A* **2004**, *70*, 062310. [CrossRef]
55. Wang, Z.M.; Wu, L.A.; Modugno, M.; Yao, W.; Shao, B. Fault-tolerant almost exact state transmission. *Sci. Rep.* **2013**, *3*, 3128. [CrossRef]
56. Mouloudakis, G.; Ilias, T.; Lambropoulos, P. Arbitrary-length X X spin chains boundary-driven by non-Markovian environments. *Phys. Rev. A* **2022**, *105*, 012429. [CrossRef]
57. Wang, Y.; Wu, J.L.; Feng, Y.K.; Han, J.X.; Xia, Y.; Jiang, Y.Y.; Song, J. Optimal control for robust photon state transfer in optomechanical systems. *Annalen der Physik* **2021**, *533*, 2000608. [CrossRef]
58. Wang, H.; Wu, L.A. Fast quantum algorithm for ec3 problem with trapped ions. *arXiv* **2014**, arXiv:1412.1722.
59. Wu, J.; Ren, F.H.; He, R.H.; Nie, S.S.; Wang, Z.M. Adiabatic speedup and quantum heat current in an open system. *Europhys. Lett.* **2022**, *139*, 48001. [CrossRef]
60. Zhang, L.C.; Ren, F.H.; Chen, Y.F.; He, R.H.; Gu, Y.J.; Wang, Z.M. Adiabatic speedup via zero-energy-change control in a spin system. *EPL (Europhys. Lett.)* **2019**, *125*, 10010. [CrossRef]
61. Jing, J.; Wu, L.A.; Yu, T.; You, J.Q.; Wang, Z.M.; Garcia, L. One-component dynamical equation and noise-induced adiabaticity. *Phys. Rev. A* **2014**, *89*, 032110. [CrossRef]
62. Wang, H.; Wu, L.A. Ultrafast adiabatic quantum algorithm for the NP-complete exact cover problem. *Sci. Rep.* **2016**, *6*, 22307. [CrossRef]
63. He, R.H.; Wang, R.; Ren, F.H.; Zhang, L.C.; Wang, Z.M. Adiabatic speedup in cutting a spin chain via zero-area pulse control. *Phys. Rev. A* **2021**, *103*, 052606. [CrossRef]
64. Ren, F.H.; Wang, Z.M.; Wu, L.A. Accelerated adiabatic quantum search algorithm via pulse control in a non-Markovian environment. *Phys. Rev. A* **2020**, *102*, 062603. [CrossRef]
65. Kingma, D.P.; Ba, J. Adam: A method for stochastic optimization. *arXiv* **2014**, arXiv:1412.6980.